Supplementary Information

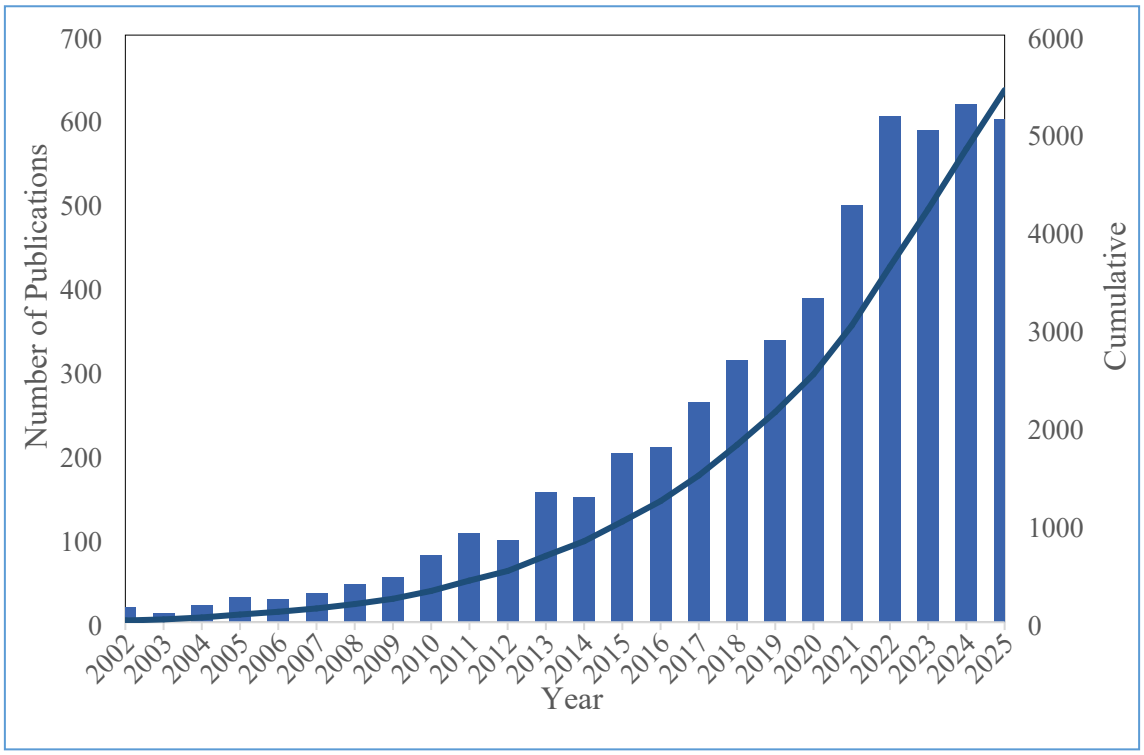

Figure S1 – Number of articles published on ScienceDirect shown when searching the keywords “Microbial Electrolysis Cell” AND “Electrode” OR “Microbial Electrolysis Cell” AND “Cathode” OR “Microbial Electrolysis Cell” AND “Anode”.

Table S1 – Summary of the studies involving Microbial Electrolysis Cells analyzed in this review paper.

Parameter	Number of studies	Percentage of the total on each category (%)
Anode Material		
Metal-based	6	11
Carbon-based	49	89
Cathode Material		
Metal-based	30	54
Carbon-based	25	46
Modifier		
Nanocomposites	29	88
Polymer	3	9
Nanocomposites + polymer	1	3
Configuration		
Single-chamber	32	58
Dual-chamber	23	42
Substrate		
Acetate	18	33
Synthetic wastewater	15	27
Industrial wastewater	6	11
Nutrient solution	6	11
Domestic wastewater	4	7
Anaerobic digestate	2	3
Glucose/sucrose	2	3
Cattle manure	1	2
Lignocellulosic hydrolyzate	1	2

Table S2 – Extra parameters reported about the electrodes used in Microbial Electrolysis Cells analyzed in this review paper.

Electrode	Electrocatalytic Activity	Conductivity & Electrical Resistance	Corrosion Resistance & Stability	Surface Area & Porosity	Biocompatibility & Biofilm Formation	Hydrophilicity	Reference
Ni-Co-P on SS & Cu	Ni-Co-P/SS had the highest catalytic activity at 3.43 mL $H_2/cm^2.g.min$, which was ~4 times higher than the bare SS (0.89 $mLH_2/cm^2.g.min$).	-	-	-	-	-	[1]
Ni-Mo Alloys on Carbon Cloth	NiMo/CC required an overpotential only 50 mV higher than a Pt/C catalyst to achieve the same current density.	The total internal resistance of the MEC was 7.6 ± 0.5 mΩ m². This was composed of: Cathode: 5.3 ± 0.5 mΩ m² (70%); Anode: 1.4 ± 0.2 mΩ m² (18%); Ohmic: 0.83 mΩ m² (11%).	-	-	-	-	[2]
CoP on Nickel	Tafel slope of	-	Stable	-	-	-	[3]

Foam	175.4 mV/dec, which was lower than Pt/C (178.4 mV/dec) indicating superior HER kinetics.		performance for over 30 days of operation, maintaining a CD_{max} of approximately 80 A/m³.				
Mo_2N Nanobelts	Required a potential of -1.0 ± 0.03 V to produce a CD of 10 A/m², (comparable to commercial Pt/C)	-	-	-	-		4
Ru on Carbon Nanotubes (Ru/CNTs)	Achieved CD of 10 mA/cm² at an overpotential of just 31 (outperforming the commercial Pt/C)	-	-	-	-	-	5
PEDOT:PSS on Carbon Felt	-	Reduced the solution resistance from 7.02 Ω to 6.44 Ω and the charge transfer resistance from 28.52 Ω to 21.05 Ω.	-	-	Showed a 220.7% increase in biofilm formation compared to control with greater abundance of electrochemically active bacteria.	The Water Contact Angle of the unmodified carbon felt was 136.5° (hydrophobic). and dropped to 0° after modification	6

						(super-hydrophilic surface).	
Fe^{2+}-modified Biochar	-	Increased electrical conductivity from 23.33 S/m to 78.65 S/m, and charge transfer resistance reduced from 10.68 Ω to 6.2 Ω, after modification.	-	-	-	-	[7]
$CoNi/CoFe_2O_4$ on Nickel Foam	-	-	The catalyst's structure remained intact after 24 days of continuous operation.	-	-	-	[8]
SS304 Mesh	-	-	Showed no evidence of corrosion after 15 operational cycles at an applied voltage of 0.9	-	-	-	[9]

			V.				
Pd on Carbon Cloth	-	Charge transfer resistance of only 15.4 Ω, dramatically lower than the bare carbon cloth control (168.2 Ω)	The electrode's peak CD dropped from 0.72 A/m² to 0.54 A/m² over 5 cycles. After applying a Nafion binder, the peak current stabilized at 0.72 A/m².	-	-	-	10
Ni_2P Nanoparticles	-	-	Tested for 11 days, longer duration than previous studies, and showed no change in performance during this period.	-	-	-	11
Spiral Wound Electrode Design	-	-	-	High specific electrode surface area of over 60 m²/m³.	-	-	12
Pt@rGO and Pt@Graphitene	-	-	-	The BET surface area was 24.40	-	-	13

				m^2/g for Pt@rGO and 10.76 m^2/g for Pt@Graphitene, and electroactive surface areas (ECSA) were 0.16 cm^2/cm^2 and 0.10 cm^2/cm^2.			
Ni- and Ce-Doped Zeolite	-	-	-	The composite material had a BET surface area of 413.47 m^2/g and an ECSA of 34.3 cm^2.	-	-	[14]
ZIF-67 Modified Bio-cathode	-	-	-	-	More abundant and thicker biofilm of sulfate-reducing bacteria on after modification	-	[15]

References

1 A. K. Chaurasia and P. Mondal, *Chemosphere*, 2022, **286**, 131728.

2 R. Rossi, J. Nicolas and B. E. Logan, *J. Power Sources*, 2023, **560**, 232594.

3 D. Liang, L. Zhang, W. He, C. Li, J. Liu, S. Liu, H.-S. Lee and Y. Feng, *Appl. Energy*, 2020, **264**, 114700.

4 S. Lu, B. Lu, G. Tan, W. Moe, W. Xu, Y. Wang, D. Xing and X. Zhu, *Biosens. Bioelectron.*, 2020, **167**, 112491.

5 L. Dai, L. Xiang, M. Zhang, Z. Wen, Q. Xu, K. Chen, Z. Zhao and S. Ci, *ChemElectroChem*, 2022, **9**, e202101584.

6 S.-G. Park, C. Rhee, D. A. Jadhav, T. Eisa, R. B. Al-Mayyahi, S. G. Shin, M. A. Abdelkareem and K.-J. Chae, *Sci. Total Environ.*, 2023, **856**, 159105.

7 X. Ji, X. Liu, W. Yang, T. Xu, X. Wang, X. Zhang, L. Wang, X. Mao and X. Wang, *Sci. Total Environ.*, 2022, **807**, 150881.

8 X. Fang, Y. Cheng, S. Li, H. Dai, Y. Zhao, X. Du, X. Ma and X. Hao, *Int. J. Energy Res.*, 2022, **46**, 340–350.

9 M. Posadas-Hernández, J. L. García-Rojas, S. Khamkure, L. García-Sánchez, T. Gutierrez-Macías, C. Morales-Morales and E. B. Estrada-Arriaga, *Int. J. Hydrog. Energy*, 2023, **48**, 495–513.

10 W. Wang, B. Zhang and Z. He, *Electrochimica Acta*, 2019, **318**, 794–800.

11 K.-Y. Kim, S. E. Habas, J. A. Schaidle and B. E. Logan, *Bioresour. Technol.*, 2019, **293**, 122067.

12 Y. Hou, R. Zhang, H. Luo, G. Liu, Y. Kim, S. Yu and J. Zeng, *Process Biochem.*, 2015, **50**, 1103–1109.

13 P. Sánchez-Peña, J. Rodriguez, D. Gabriel, J. A. Baeza, A. Guisasola and M. Baeza, *Int. J. Hydrog. Energy*, 2022, **47**, 15397–15409.

14 J. Wang, Y. Li, M. Liu, Z. Li, X. Gao and D. Yang, *ChemPlusChem*, 2020, **85**, 2290–2297.

15 J. Dai, Z. Huang, H. Zhang, H. Shi, S. R. B. Arulmani, X. Liu, L. Huang, J. Yan and T. Xiao, *Sci. Total Environ.*, 2023, **856**, 158839.